Second-harmonic generation in single-mode integrated waveguides based on mode-shape modulation

Ashutosh Rao, Jeff Chiles, Saeed Khan, Seyfollah Toroghi, Marcin Malinowski, Guillermo Fernando Camacho-González, and Sasan Fathpour

Citation: Appl. Phys. Lett. **110**, 111109 (2017); doi: 10.1063/1.4978696
View online: http://dx.doi.org/10.1063/1.4978696
View Table of Contents: http://aip.scitation.org/toc/apl/110/11
Published by the American Institute of Physics

Second-harmonic generation in single-mode integrated waveguides based on mode-shape modulation

Ashutosh Rao,[1,a)] Jeff Chiles,[1,a),b)] Saeed Khan,[1] Seyfollah Toroghi,[1,c)] Marcin Malinowski,[1] Guillermo Fernando Camacho-González,[1] and Sasan Fathpour[1,2,d)]
[1]*CREOL, The College of Optics and Photonics, University of Central Florida, Orlando, Florida 32816, USA*
[2]*Electrical Engineering and Computer Engineering Department, University of Central Florida, Orlando, Florida 32816, USA*

(Received 19 January 2017; accepted 4 March 2017; published online 17 March 2017)

Second-harmonic generation is demonstrated using grating-assisted quasi-phase matching, based on waveguide-width modulation or mode-shape modulation. Applicable to any thin-film integrated second-order nonlinear waveguide, the technique is demonstrated in compact lithium niobate ridge waveguides. Fabricated devices are characterized with pulsed-pumping in the near-infrared, showing second-harmonic generation at a signal wavelength of 784 nm and propagation loss of 1 dB/cm. *Published by AIP Publishing*. [http://dx.doi.org/10.1063/1.4978696]

Optical three-wave mixing,[1,2] utilizing the second-order nonlinearity ($\chi^{(2)}$) of non-centrosymmetric materials, has enabled the generation of coherent light over a wide range of frequencies from the ultraviolet to the infrared in different material systems. Efficient three-wave mixing processes, such as second-harmonic generation (SHG), sum- and difference-frequency generation (SFG/DFG) and spontaneous parametric down conversion, require optical phase matching, which is a compensation between the different wavevectors of the interacting waves. Nonlinear frequency conversion is anticipated to be significantly more efficient in integrated nonlinear waveguides than in bulk nonlinear crystals, due to an increase in the nonlinear overlap between the interacting waves.[2,3] Consequently, several approaches have been explored for optical phase matching for frequency conversion using three-wave mixing in waveguides. Arguably, the most popular approach has been quasi-phase matching (QPM), where the phase mismatch between the interacting waves is periodically compensated. The most successful implementation of QPM has been in periodically poled lithium niobate (PPLN) waveguides.[4–6]

An alternative poling-free implementation for integrated QPM uses periodic gratings.[7–10] Grating-assisted quasi-phase matching (GA-QPM) mimics the concept and benefits the more established periodic-poling method, but with more relaxed fabrication demands and, of course, applicability to materials that cannot be inherently poled. Generally, a net nonlinear gain for GA-QPM based frequency conversion is achieved via periodic spatial perturbation of waveguide geometrical parameters, for example, mode-shape modulation (MSM), exploited in this work. This is in contrast to periodic poling, in which the sign of the nonlinearity is entirely and periodically reversed in the crystal. Previous demonstrations of GA-QPM include GaAs[8,9] and titanium-diffused lithium niobate ($LiNbO_3$ or LN) waveguides.[10] A similar approach has also been previously applied to four-wave mixing in integrated silicon waveguides.[11]

Meanwhile, our team has pioneered a platform for thin-film $LiNbO_3$.[12] The advantage of the thin-film technology, compared to a conventional titanium-diffused waveguide, is the high-contrast waveguides formed by bonding 300 to 600 nm of $LiNbO_3$ (with a refractive index of ~2.16) on a silicon dioxide (SiO_2 with an index of ~1.48) bottom-cladding layer and rib-loading it with an index-matching material (e.g., silicon nitride, SiN), for lateral confinement. High-performance electrooptic modulators[13,14] and PPLN waveguides for SHG[6] have been demonstrated on the platform.

In this work, a variation of GA-QPM is applied to our thin-film $LiNbO_3$ waveguide technology to achieve SHG. The approach, which may be also called mode-shape modulation (MSM), relies on periodically modulating the width of the SiN rib on top of the $LiNbO_3$ thin film. The width modulation conveniently provides QPM, while the challenges of etching or poling are avoided (see Fig. 1(a)). Thus, the nonlinear effect is exclusively obtained from the modulation of the nonlinear mode overlap integral between the fundamental (pump) and generated second-harmonic (SH) waves, and mediated by the refractive index perturbation. Another advantage over the aforementioned works on GaAs and titanium-diffused waveguides is the shallow etching of the thin (400 nm) SiN rib layer, thanks to the tight mode confinement of the high-contrast waveguides. To avoid grating-induced losses from coupling into higher order modes, a ridge waveguide structure is adopted, utilizing a sinusoidal width perturbation in the rib, which is kept in single-mode operation for both the pump and SH wavelengths.

The fabricated waveguides are formed by depositing a 400-nm-tall rib of SiN on a 600-nm thin film of *X*-cut LN, surrounded by SiO_2 bottom and top clads. The width of the SiN rib sinusoidally varies from 855 nm to 1095 nm, with a period around 5.5 μm, as dictated by the phase mismatch, according to COMSOL™ simulations. Only the SiN film is patterned, i.e., the LN film is unetched to avoid etch-induced losses,[6,12–14] as shown in Fig. 1(a). Thus, there is no spatial perturbation of the *d* tensor, and the nonlinear effect is exclusively due to the

[a)]A. Rao and J. Chiles contributed equally to this work.
[b)]Now at National Institute of Standards and Technology (NIST), Boulder, Colorado 80305, USA.
[c)]Now at Partow Technologies LLC, Orlando, Florida 32816, USA.
[d)]Electronic mail: fathpour@creol.ucf.edu

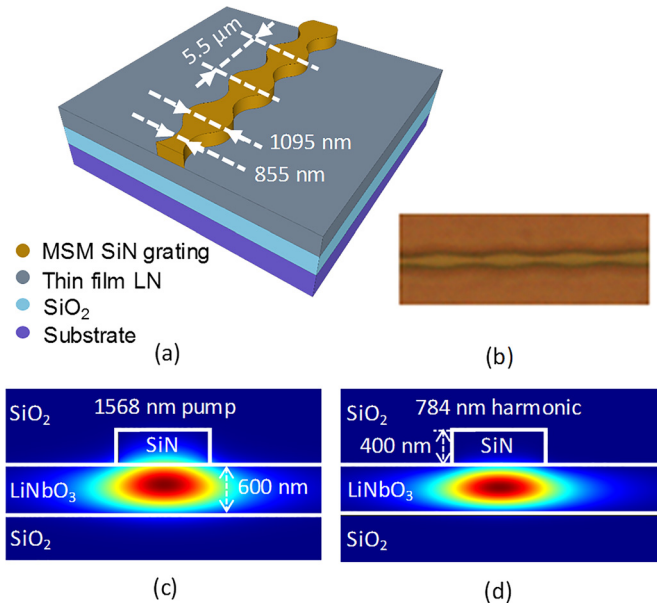

FIG. 1. (a) Concept of the GA-QPM ridge waveguide used in this work, showing the longitudinally varied waveguide width following a sinusoidal pattern (exaggerated in its magnitude for visibility). The minimum and maximum widths of the grating are also indicated; (b) top-view optical micrograph of a fabricated waveguide; and (c) and (d) intensity profile of the fundamental and second-harmonic TE modes of the waveguide at a grating width of 1095 nm.

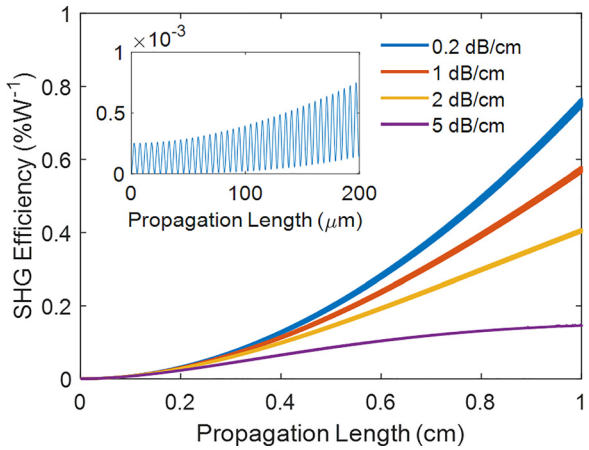

FIG. 2. SHG conversion efficiency versus propagation length for the MSM numerical simulation for different propagation loss values. The inset presents the associated normalized SH field amplitude along with the oscillations that are present but too small to be discernible in the main figure.

width modulation of the SiN rib. The design is phase-matched for transverse-electric (TE) modes, thus ensuring that the SHG process is mediated by the largest nonlinear coefficient of LN, viz., d_{33}. An optical micrograph of the top view of a fabricated waveguide is provided in Fig. 1(b). The transverse TE modes of the pump and SH waves at a grating width of 1095 nm are shown in Figs. 1(c) and 1(d).

The GA-QPM thin film LN waveguides are numerically investigated using the local normal-mode expansion (LNME),[15] where the eigenmodes of the local spatial structure of the waveguide are used for the expansion. The corresponding coupled-mode equations for the normalized field amplitudes during SHG assume the form

$$\frac{d}{dz}a_{2\omega}(z) = -i(a_{\omega}(z))^2 e^{i\Delta\beta_0 z} f(z) - \frac{\alpha_{2\omega}}{2}a_{2\omega}(z), \quad (1a)$$

$$\frac{d}{dz}a_{\omega}(z) = -i a_{\omega}(z) a_{2\omega}{}^{*}(z) e^{-i\Delta\beta_0 z} f^{*}(z) - \frac{\alpha_{\omega}}{2}a_{\omega}(z), \quad (1b)$$

where $a_{2\omega}(z)$ and $a_{\omega}(z)$ are the normalized field amplitudes of the signal (SH) and the pump at frequencies 2ω and ω, respectively, and $\alpha_{2\omega}$ and α_{ω} are the corresponding averaged waveguide propagation losses. $\Delta\beta_0$ is the phase mismatch between the signal and the pump waves, averaged over one period. $f(z)$ is a nonlinear coupling coefficient that captures the effect of the periodic modulation of the waveguide on both the transverse field overlaps at ω and 2ω. Further details can be found in Ref. 15.

The quadratic SHG process is simulated for the aforementioned waveguide dimensions. The normalized SHG conversion efficiency is presented in Fig. 2, and is a figure of merit of the nonlinear waveguide, and is independent of the input optical power, and the mode of operation (pulsed or continuous wave (CW)). $f(z)$ is evaluated numerically using an eigenmode solver by Lumerical Solutions. The first-order term in the Fourier series expansion of $f(z)$ cancels out the $exp(\pm i\Delta\beta_0 z)$ phase terms in Eqs. (1a) and (1b), hence driving the nonlinear growth of the SH field, while the constant term in the series expansion results in fast oscillations of the SH field. The propagation loss is varied from 0 to 5 dB/cm, illustrating the effect of propagation loss on the SHG process. The inset in Fig. 2 displays the fast oscillations of the SH field amplitude.

The normalized CW conversion efficiency is extracted to be $\sim$0.8% $W^{-1}\,cm^{-2}$. A similar evaluation of the nonlinear effect using 500-fs-long transform-limited hyperbolic secant pulses for the pump yields the same conversion efficiency by adapting the analytical model described in Ref. 16 for grating-assisted quasi-phase matching. The group-velocity mismatch-induced pulse walk-off leads to SHG pulse durations around 4 ps in 5 mm long waveguides for the 500 fs input. It is stressed, however, that this theoretical estimation is based on the assumption of transform-limited input pulses, which may not necessarily be applicable to the input source employed in the experiments (Fig. 3(a)).

It is noted that while the above simulated efficiency is lower than what has been achieved in PPLN ($\sim$40% $W^{-1}\,cm^{-2}$),[17,18] the challenges of periodically poling thin-film devices in terms of required short periodicities[6] and applicability of the proposed technique to $\chi^{(2)}$ material systems that cannot be poled must be stressed.

Finally, we remark that the physical dimensions of the waveguide strongly influence the nonlinear SHG process. Varying the height of the LN film affects both the grating-induced waveguide propagation losses, $a_{2\omega}(z)$ and $a_{\omega}(z)$, and the magnitude of the first Fourier series coefficient of $f(z)$ that drives the nonlinear process. The extent of the width modulation has a similar effect on these factors. A larger width modulation increases the strength of the nonlinear coupling coefficient, but at the cost of increased propagation losses. Thus, a balance must be maintained between the propagation losses and the Fourier series coefficients of $f(z)$.

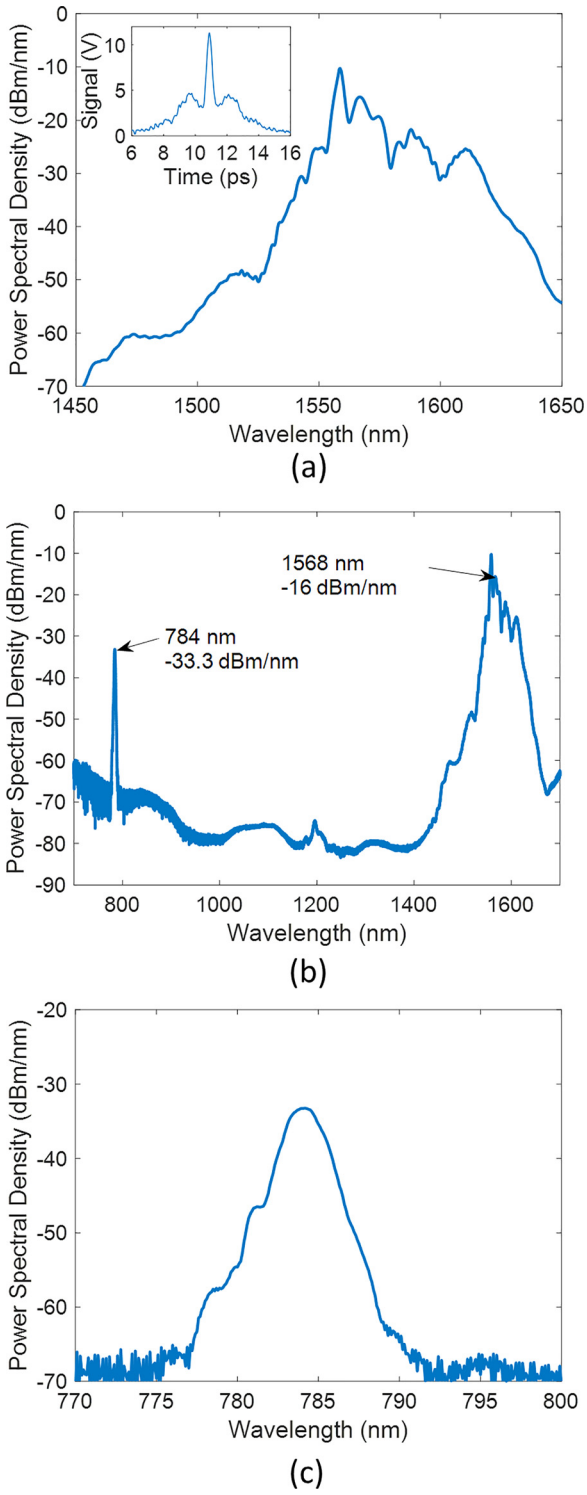

FIG. 3. (a) Pulsed pump input spectrum and autocorrelation (inset); (b) OSA trace of the output; and (c) SH signal generated around 784 nm.

The 4.9-mm-long waveguides were characterized by pulsed-pumping at a 100 MHz repetition rate with a 500 fs pulse duration source, with a 7 ps pedestal (see the inset of Fig. 3(a)). The spectrum is centered at 1560 nm, with an average power of 84 mW (Fig. 3(a)). The source light was coupled on and off the chip through lensed fibers, with an estimated coupling loss of 6.5 dB/facet. A fiber-based polarization controller was used at the input to align the polarization in the horizontal direction, corresponding to the *Z*-axis of the LN film and the TE mode of the waveguide. The output light from the waveguide was collected and fed to an optical spectrum analyzer (OSA) to determine the phase-matching wavelength for a given period. Based on the total fiber to fiber insertion loss of 13.5 dB at the pump wavelength, a low propagation loss of 1 dB/cm is estimated, due to the low loss from the SiN grating and not etching the LN layer for lateral confinement. An OSA trace, showing the generated SH signal at 784 nm, is shown in Figs. 3(b) and 3(c), with a peak power spectral density of −33.3 dBm/nm for the signal. The pump shows a power spectral density of −16 dBm/nm at the corresponding phase-matched wavelength of 1568 nm, indicating a penalty of −17.3 dB from the SHG process. Differences between the coupling efficiency for the pump and signal waves into the tapered fiber may influence this value slightly. A plot of integrated pump power versus integrated output power at the harmonic tone, shown in Fig. 4, confirms the quadratic relationship consistent with the SHG process, with a slope of 2.18 for a straight-line fit.

The generated signal at 784 nm has a linewidth of ∼2.2 nm. Such a narrow linewidth is governed by the phase matching conditions of any involved nonlinear processes, primarily SHG. Due to the broad spectrum of the input pulse, it is also possible that there is a degree of contribution from sum-frequency generation (SFG). Meanwhile, it should be noted that the harmonic tone cannot be generated by mode-matching processes, since the waveguide design is single-mode at both the pump and signal wavelengths.

Assuming the aforementioned 4 ps SHG pulse widths for a transform-limited input source, and accounting for only the corresponding spectral region of the pump, it is possible to extract a very crude nonlinear conversion efficiency of $\sim 1\%/(\mathrm{W\,cm^2})$ from the presented data. However, an accurate estimate of the experimental conversion efficiency would require good understanding of the spectral phase of the input pulse measured by methods such as frequency-resolved optical gating (FROG). This complication is in addition to the aforementioned possible contribution from SFG. Future investigations with a CW input will allow attaining a more accurate experimental normalized conversion efficiency for the reported method.

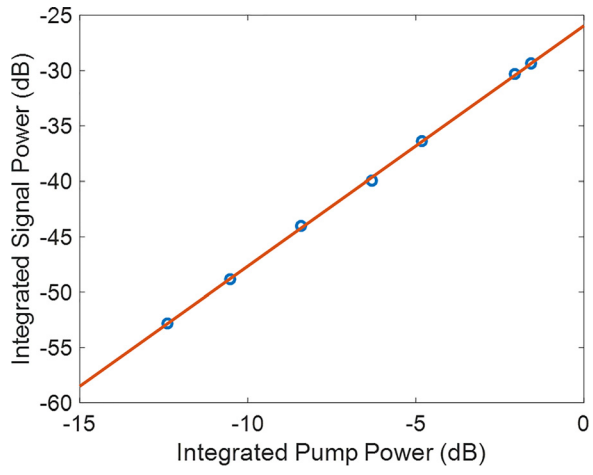

FIG. 4. Measured pump power vs. signal power, showing the quadratic slope of 2.18 (fitted line).

It should be finally discussed that the conversion efficiency could be increased by employing a higher-refractive-index rib-loading material to allow faster compression of the mode. Additionally, there may be more optimized alternative width modulation patterns, which can simultaneously achieve low grating-induced losses and high SH conversion efficiency.

In conclusion, waveguide width or mode-shape modulation is employed to obtain poling-free quasi-phase matching in thin-film lithium niobate. Second harmonic generation is demonstrated at a signal wavelength of 784 nm, utilizing near-infrared pulsed pumping. A low propagation loss of ~1 dB/cm is measured. This implementation is directly applicable to other conventional second-order nonlinear integrated waveguide platforms, notably material systems such as compound semiconductors which cannot be periodically poled.

This project is being supported by the U.S. Office of Naval Research (ONR) Young Investigator Program and the U.S. Defense Advanced Research Projects Agency (DARPA). The views, opinions, and/or findings expressed are those of the author and should not be interpreted as representing the official views or policies of the Department of Defense or the U.S. Government.

[1]R. W. Boyd, *Nonlinear Optics* (Academic Press, 2003).
[2]M. M. Fejer, Phys. Today **47**(5), 25 (1994).
[3]M. L. Bortz, Ph.D. thesis, Stanford University, 1994.
[4]W. Sohler and H. Suche, Appl. Phys. Lett. **33**, 518 (1978).
[5]K. R. Parameswaran, R. K. Route, J. R. Kurz, R. V. Roussev, M. M. Fejer, and M. Fujimura, Opt. Lett. **27**, 179 (2002).
[6]A. Rao, M. Malinowski, A. Honardoost, J. R. Talukder, P. Rabiei, P. Delfyett, and S. Fathpour, Opt. Express **24**, 29941 (2016).
[7]S. Somekh and A. Yariv, Appl. Phys. Lett. **21**, 140 (1972).
[8]J. P. van der Ziel, M. Ilegems, P. W. Foy, and R. M. Mikulyak, Appl. Phys. Lett. **29**, 775 (1976).
[9]A. Hayat, Y. Elor, E. Small, and M. Orenstein, Appl. Phys. Lett. **92**, 181110 (2008).
[10]B. Jaskorzynska, G. Arvidsson, and F. Laurell, Proc. SPIE **0651**, 221–228 (1986).
[11]J. B. Driscoll, N. Ophir, R. R. Grote, J. I. Dadap, N. C. Panoiu, K. Bergman, and R. M. Osgood, Opt. Express **20**, 9227 (2012).
[12]P. Rabiei, J. Ma, S. Khan, J. Chiles, and S. Fathpour, Opt. Express **21**, 25573 (2013).
[13]A. Rao, A. Patil, J. Chiles, M. Malinowski, S. Novak, K. Richardson, P. Rabiei, and S. Fathpour, Opt. Express **23**, 22746 (2015).
[14]A. Rao, A. Patil, P. Rabiei, A. Honardoost, R. DeSalvo, A. Paolella, and S. Fathpour, Opt. Lett. **41**, 5700 (2016).
[15]T. Isoshima and K. Tada, IEEE J. Quantum Electron. **33**, 164 (1997).
[16]E. Sidick, A. Knoesen, and A. Dienes, J. Opt. Soc. Am. B **12**, 1704 (1995).
[17]F. Généreux, G. Baldenberger, B. Bourliaguet, and R. Vallée, Appl. Phys. Lett. **91**, 231112 (2007).
[18]S. Sonoda, I. Tsuruma, and M. Hatori, Appl. Phys. Lett. **70**, 3078 (1997).